Substituted C_{60} Molecules: A Study in Symmetry Reduction

Bruce Chase* and Paul J. Fagan

Contribution from the Central Research and Development Department, Experimental Station, E. I. du Pont de Nemours and Company, Inc., P.O. Box 80328, Wilmington, Delaware 19880-0328.
Received September 30, 1991

Abstract: The Raman spectra of various organometallic complexes of C_{60} have been obtained and compared to the Raman spectrum of unsubstituted C_{60}. The reduction in symmetry of the molecular system is clearly demonstrated by the appearance of vibrational modes which were symmetry forbidden in I_h symmetry. The high-frequency C_{60} modes are shifted to slightly lower frequency, indicating a weakening of the C–C bonds. This is thought to arise from metal to C_{60} π backbonding.

The recent discovery of a synthetic route providing reasonable quantities of the C_{60} molecule[1] has enabled many physical and chemical characterization studies of this high-symmetry molecular system. The data from infrared[2] and Raman spectroscopies[3] as well as NMR[4] spectroscopy have established the icosahedral (I_h) symmetry of the molecular system. Excluding possible solid-state effects, there are 174 vibrational modes for a 60-atom molecule ($3N - 6$), but under I_h symmetry only 4 vibrations are allowed in the infrared spectrum and 10 in the Raman spectrum. The four infrared active modes have T_{1u} symmetry and are triply degenerate. The Raman active modes consist of two singly degenerate A_{1g} modes and eight 5-fold degenerate H_g modes. In the infrared spectrum many weaker features are observed at an order of magnitude lower intensity. These modes could arise from isotopic or solid-state effects breaking the symmetry. In the Raman spectrum no such lower intensity modes are observed. If the symmetry of the molecular system could be reduced without significantly perturbing the normal mode structure of the fullerene, the degeneracy of some of these modes might be removed. In addition, vibrational modes that were silent under I_h symmetry could become allowed. Surface-enhanced Raman spectra of C_{60} adsorbed onto a gold surface[5] have shown a dramatic increase in the number of observed vibrational modes in the Raman spectrum, and the additional features have been attributed to distortion of the molecular geometry, a reduction in symmetry, and electronic effects or a combination of all three. The recent synthesis of several metallo–organic complexes comprising C_{60} and various platinum, palladium, and nickel systems[6,7,14] provides a means of testing this hypothesis. In this study, we examined the effect on the Raman spectrum of metal substitution on the C_{60} sphere. It is found that Raman spectroscopy is a valuable tool for characterizing C_{60} derivatives as well as demonstrating the role of symmetry in the observed features of the spectrum.

Experimental Section

The synthesis of the various nickel, palladium, and platinum complexes is described elsewhere.[6,7,14] The $Pt(PPh_3)_2Cl_2$ and $Pt(PEt_3)_2Cl_2$ were prepared according to literature procedures.[8-10]

Table I

$Pt(PPh_3)_2C_{60}$		C_{60}		$Pd(PPh_3)_2C_{60}$	
freq, cm^{-1}	intensity[a]	freq, cm^{-1}	intensity[a]	freq, cm^{-1}	intensity[a]
265	0.65			266	0.50
271	0.42	272 (H_g)	0.86	278	0.03
291	0.33			290	0.34
348	0.05				
377	0.61			374	0.98
434	0.11	432 (H_g)	0.13	431	0.14
448	0.23			444	0.38
490	0.66	485 (A_g)	sh[b]	490	0.83
		495 (A_g)	1.00		
507	0.19			504	0.32
529	0.09	534	0.07	530	0.35
552	0.75			543	1.40
563	0.20	566	0.08	567	0.20
581	0.75			579	0.83
671	0.07			670	0.15
709	0.18	710 (H_g)	0.06	709	0.56
722	0.41			716	0.51
746	0.37			743	0.38
759	0.38	772 (H_g)	0.20	758	0.24
774	0.12			774	0.13
948	0.07			951	0.11
971	0.05				
1003	0.16[c]			1002	0.25[c]
1034	0.04[c]				
1077	0.03				
1097	0.08	1100 (H_g)	0.11	1096	0.14
1177	0.05			1189	0.08
1286	0.06	1249 (H_g)	0.09	1295	0.10
1423	0.14	1425 (H_g)	0.05	1423	0.27
1461	1.00	1468 (A_g)	0.92	1461	1.00
1552	0.04			1549	0.02
1573	0.12	1574 (H_g)	0.12	1573	0.19
1588	0.04[c]			1587	0.05[c]
3058	0.04[c]			3058	0.03[c]

[a] Intensities (peak height) are relative to the strongest observed mode. [b] Shoulder. [c] PPh_3 modes.

FT-Raman spectra were acquired on a Nicolet 800 interferometer equipped with a Raman accessory bench operating in a 180° backscattering configuration. The apodized spectral resolution was 2.3 cm^{-1}, and 250 scans were co-added to improve the signal to noise ratio. The incident power on the samples was 40 mW in all cases except the $Pt(PPh_3)_2Cl_2$, which required 250 mW. The C_{60} sample was prepared as described in the literature[1] and purified by alumina column chromatography. All samples were examined in glass capillaries which were loaded under nitrogen and sealed. In no case was there evidence of thermal degradation or photochemical reaction over the course of spectral acquisition.

(1) (a) Krätschmer, W.; Fostiropoulos, K.; Huffman, D. R. *Chem. Phys. Lett.* **1990**, *170*, 167. (b) Krätschmer, W.; Lamb, L. D.; Fostiropoulos, K.; Huffman, D. R. *Nature* **1990**, *347*, 345.
(2) Hare, J.; Dennis, J.; Kroto, H.; Taylor, R.; Allaf, A.; Balm, S.; Walton, D. *Chem. Commun.* **1991**, 412.
(3) Bethune, D. S.; Meijer, G.; Tang, W. C.; Rosen, H. *Chem. Phys. Lett.* **1990**, *174*, 219.
(4) Johnson, R.; Meijer, G.; Bethune, D. *J. Am. Chem. Soc.* **1990**, *112*, 8985.
(5) Garrell, R. L.; Herne, T. M.; Szafranski, C. A.; Diederich, F.; Ettl, F.; Whetten, R. L. *J. Am. Chem. Soc.* **1991**, *113*, 6302.
(6) Fagan, P. J.; Calabrese, J. C.; Malone, B. *Science* **1991**, *252*, 1160.
(7) Fagan, P. J. Unpublished results.
(8) Royle, J. R.; Slade, P. E.; Jonassen, H. B. *Inorg. Synth.* **1960**, *6*, 218.
(9) Parshall, G. W. *Inorg. Synth.* **1970**, *12*, 27.
(10) Jensen, K. A. *Z. Anorg. Allg. Chem.* **1936**, *229*, 265.

0002-7863/92/1514-2252$03.00/0

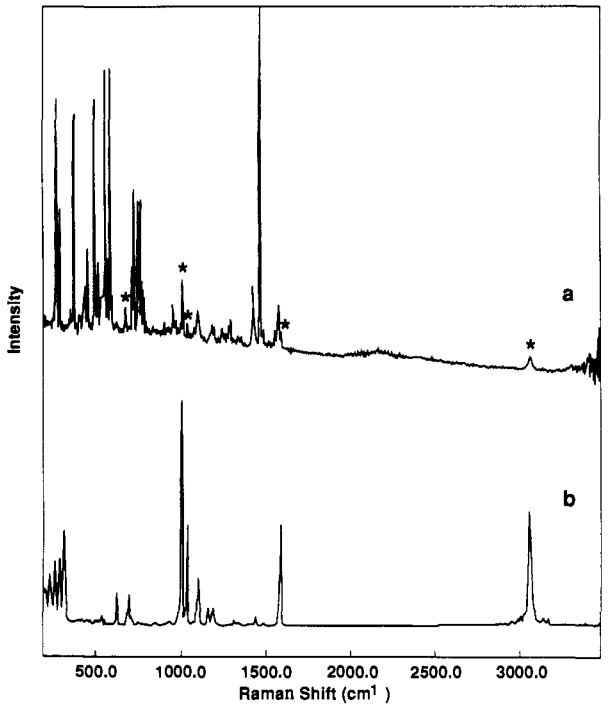

Figure 1. (a) FT-Raman spectrum of $Pt(PPh_3)_2(\eta^2\text{-}C_{60})$. (b) FT-Raman spectrum of $Pt(PPh_3)_2Cl_2$.

Results

The X-ray crystal structure of $Pt(PPh_3)_2(\eta^2\text{-}C_{60})$ has shown that there is only slight distortion of the C_{60} sphere upon bonding to the platinum.[6] The two carbons involved in the bonding to the platinum are slightly pulled out of the C_{60} sphere, but the overall perturbation is small, leading to only minor changes in the expected normal modes of vibration of the carbon system. The normal modes of vibration are a function of geometry, mass, and force constant. The X-ray data show no evidence of significant distortion to a more ellipsoidal shape, similar to C_{70}. As long as the coupling between the platinum phosphine unit and the C_{60} unit is weak, the mass effects on the C_{60} modes should be small and the spectrum could be represented as a simple addition of the spectrum of C_{60}, the spectrum of a platinum bis(phosphine) group, and the spectral features associated with platinum–carbon stretching motions. However, the symmetry of the molecular system has been reduced to C_1 for the full molecule (C_{2v} if the phenyl groups are ignored). For either symmetry the degeneracies of all vibrational modes have been removed and all modes become symmetry allowed in Raman scattering. Since the observed distortions of the C_{60} geometry are relatively minor, the change in vibrational frequencies due to mass effects should be small. However, even if the perturbations of the normal mode structure are small, the force constants of the vibrations are likely to be changed by electronic effects; i.e., the bonding of the platinum to the C_{60} could change the electronic distribution within the σ and/or π system.

Raman spectra were obtained of both C_{60} and the platinum complex $Pt(PPh_3)_2(\eta^2\text{–}C_{60})$ using FT-Raman[11] techniques. It should be noted that in both the infrared and Raman spectra of C_{60} the line widths are extremely narrow, on the order of several cm^{-1}. To obtain accurate relative intensity information, which is not distorted by the instrument line shape function, resolutions of 2 cm^{-1} or less are mandatory. The Raman scattering of both C_{60} and the platinum complex is extremely strong as evidenced by large Raman intensities at low laser power, which is consistent with the high degree of polarizability of the C_{60} sphere. For excitation at 1.064 μm, there should be minimal contribution from a resonance Raman effect and the strong scattering from the C_{60} part of the complex should dominate the spectrum. The Raman

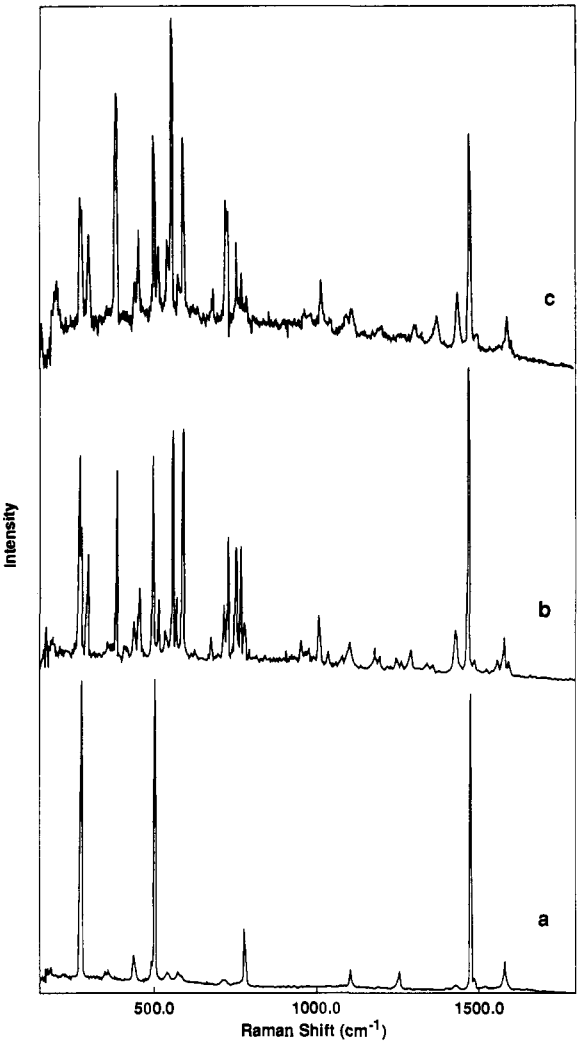

Figure 2. (a) FT-Raman spectrum of C_{60}. (b) FT-Raman spectrum of $Pt(PPh_3)_2(\eta^2\text{-}C_{60})$. (c) FT-Raman spectrum of $Pd(PPh_3)_2(\eta^2\text{-}C_{60})$.

bands due to the phosphine groups should be weak in comparison. This is confirmed in Figure 1, where the FT-Raman spectra of $Pt(PPh_3)_2(\eta^2\text{-}C_{60})$ (a) and a model compound $Pt(PPh_3)_2Cl_2$ (b) are shown. In Figure 1b the intensity of the aromatic C–H stretch at 3080 cm^{-1} is one of the stronger modes in the spectrum. These data were acquired with 200 mW of power to compensate for the weaker scattering relative to the C_{60} samples. Using the intensity of the band at 3080 cm^{-1} as an internal standard, it is clear that only a few weak bands in the spectrum of the platinum–C_{60} complex are due to the phosphine groups. These modes are marked with an asterisk and are labeled in Table I. There are additional low-frequency modes in the 300-cm^{-1} region some of which are due to Pt–Cl stretches and would not be present in the spectrum of the $Pt(PPh_3)_2(\eta^2\text{-}C_{60})$ complex. Figure 2 shows the FT-Raman spectra of the $Pt(PPh_3)_2(\eta^2\text{-}C_{60})$ and $Pd(PPh_3)_2(\eta^2\text{-}C_{60})$ complexes along with the spectrum of pure C_{60}. The change in metal from platinum to palladium in the complex has had little effect on the spectrum. This confirms that the large majority of the spectral features are due to symmetry-reduced C_{60} vibrational modes. The phosphine ligand modes which are expected to shift with changing metal centers are weak relative to the C_{60} modes, and small shifts cannot be detected. The observed frequencies are given in Table I along with symmetry designations for the C_{60} modes. There is a noticeable difference in some of the relative intensities of the C_{60} modes when compared to previous studies.[12] We believe this is due to a dependence on

(11) Chase, B. *J. Am. Chem. Soc.* **1986**, *108*, 7485.

(12) Bethune, D. S.; Meijer, G.; Tang, W. C.; Rosen, H. J.; Golden, W.; Seki, H.; Brown, C.; de Vries, M. S. *Chem. Phys. Lett.* **1991**, *179*, 181.

Table II

C_{60}		$(Et_3P)_2NiC_{60}$		$(Et_3P)_2PdC_{60}$		$(Et_3P)_2PtC_{60}$	
freq, cm^{-1}	intensity[a]	freq, cm^{-1}	intensity[a]	freq, cm^{-1}	intensity[a]	freq, cm^{-1}	intensity[a]
		169	0.17	168	0.13		
				220	0.05		
272 (H_g)	0.86	270	0.47	270	0.47	270	0.56
				289	0.27	288	0.23
		380	0.39	375	0.64	377	0.61
432 (H_g)	0.13	429	0.19	430	0.18	430	0.24
		446	0.28	443	0.40	446	0.37
485	(sh)	489	0.53	488	0.65	488	0.68
495 (A_g)	1.00	503	0.19	503	0.18	511	0.17
		528	0.33	528	0.38	528	0.21
534	0.07	545	0.67	540	0.93	546	0.91
		562	0.15	564	0.20	561	0.24
566	0.08	579	0.67	578	0.82	579	0.98
				669	0.16	670	0.12
710 (H_g)	0.06	708	0.47	709	0.65	708	0.39
		717	0.50				
		741	0.56	740	0.62	721	0.43
772 (H_g)	0.20	760	0.31	759	0.29	760	0.45
						773	0.28
		948	0.14	947	0.13	946	0.19
		1033	0.14	1033	0.20	1037	0.16
1100 (H_g)	0.11	1080	0.08	1080	0.13		
		1176	0.08	1177	0.07	1170	0.11
1249 (H_g)	0.09	1252	0.11	1251	0.11	1252	0.14
		1283	0.08	1289	0.09	1279	0.10
				1351	0.07		
1425 (H_g)	0.05	1420	0.28	1422	0.36	1420	0.29
1468 (A_g)	0.92	1458	1.00	1459	1.00	1458	1.00
				1475	0.09		
		1547	0.11	1547	0.07	1548	0.11
1574 (H_g)	0.12	1570	0.19	1570	0.20	1569	0.19

[a] Intensities (peak height) are relative to the strong mode at 1468 cm^{-1}.

excitation frequency. Earlier studies done with visible excitation at 514.5 nm most likely involved some degree of resonant or preresonant enhancement, whereas Raman spectra obtained at 1.064 μm are clearly removed from the resonance condition. Current work is directed toward obtaining the resonance excitation profiles for C_{60} and will clarify this point. Clearly the symmetry reduction provides for many more allowed vibrational modes of C_{60}. In fact, the mode at 774 cm^{-1}, which is 5-fold degenerate under I_h symmetry for C_{60} (Figure 2a), shows a splitting into five components for the $Pt(PPh_3)_2(\eta^2\text{-}C_{60})$ complex (Figure 2b). Figure 2c shows the spectrum for the $Pd(PPh_3)_2(\eta^2\text{-}C_{60})$ system.

Similar complexes have now been synthesized using triethylphosphine rather than triphenylphosphine as the ligand. The FT-Raman spectra of $Ni(PEt_3)_2(\eta^2\text{-}C_{60})$, $Pd(PEt_3)_2(\eta^2\text{-}C_{60})$, and $Pt(PPh_3)_2(\eta^2\text{-}C_{60})$ are shown in Figure 3, and the observed frequencies and relative intensities are given in Table II. There are minor intensity differences when compared to the data in Figure 2, but the main pattern of new bands and splittings remains the same, thus confirming similar structures. The major difference is the absence of the weak modes attributed to the phenylphosphine ligands. The scattering from the triethylphosphine groups is even weaker than for the triphenylphosphine groups (using $Pt(PEt_3)_2Cl_2$ as the model compound), and no new ligand modes are observed. The totally symmetric (A_g) modes in C_{60} do not exhibit any splitting in the complexes, as expected. In agreement with the SERS study[5] we observe a general lowering in frequency of the C_{60} vibrations upon complexation, indicative of either a loss in electron density from the C_{60} due to donation of π electron density to the metal or metal-to-molecule backbonding to the π^* orbitals. Current studies on the electrochemical behavior of $Pt(PPh_3)_2(\eta^2\text{-}C_{60})$ favor the backdonation hypothesis since the reduction

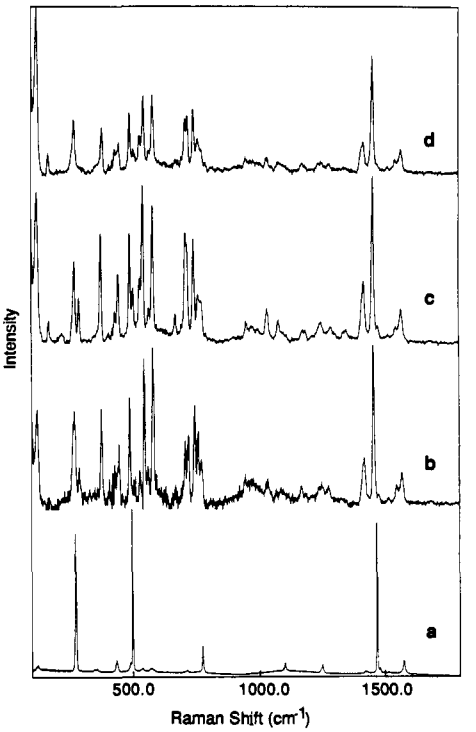

Figure 3. (a) FT-Raman spectrum of C_{60}. (b) FT-Raman spectrum of $Pt(PEt_3)_2(\eta^2\text{-}C_{60})$. (c) FT-Raman spectrum of $Pd(PEt_3)_2(\eta^2\text{-}C_{60})$. (d) FT-Raman spectrum of $Ni(PEt_3)_2(\eta^2\text{-}C_{60})$.

Table III

C_{60}		$((Et_3P)_2Ni)_6C_{60}$		$((Et_3P)_2Pd)_6C_{60}$		$((Et_3P)_2Pt)_6C_{60}$	
freq, cm^{-1}	intensity[a]	freq, cm^{-1}	intensity[a]	freq, cm^{-1}	intensity[a]	freq, cm^{-1}	intensity[a]
				221	0.17		
272 (H_g)	0.86	266	0.11	266	0.23	265	0.32
				311	0.56	316	0.49
		340	0.16				
432 (H_g)	0.13	422	0.19	423	0.28	423	0.36
				459	0.95		
485	(sh)						
495 (A_g)	1.00	479	0.90	480	0.29	479	0.99
		536	0.73	532	1.11	534	0.85
534	0.07			546	0.18	545	0.30
		550	0.14	557	0.47	555	0.38
		572	0.66			578	0.76
566	0.08	625	0.09	624	0.11	591	0.34
		686	0.11	689	0.22	689	0.31
710 (H_g)	0.06	719	0.69	705	0.52		
				730	0.14	724	0.51
		745	1.00	745	1.00	750	1.00
772 (H_g)	0.20	781	0.10	781	0.17	788	0.25
		798	0.04			802	0.21
		819	0.05	821	0.09	823	0.22
		1037	0.04	1034	0.10	1034	0.08
		1070	0.16	1075	0.24	1067	0.22
1100 (H_g)	0.11	1089	0.20	1086	0.19	1082	0.24
1249 (H_g)	0.09	1247	0.23	1260	0.24	1243	0.39
		1306	0.05				
		1333	0.15	1346	0.41	1331	0.29
						1346	0.29
1425 (H_g)	0.05	1357	0.15	1372	0.52		
1468 (A_g)	0.92	1413	0.62	1421	1.08	1412	0.72
		1460	0.02	1457	0.06	1457	0.04
		1518	0.34	1521	0.56	1521	0.43
1574 (H_g)	0.12	1555	0.05	1560	0.08	1561	0.12

[a] Intensities (peak height) are relative to the strong mode at 475 cm^{-1}.

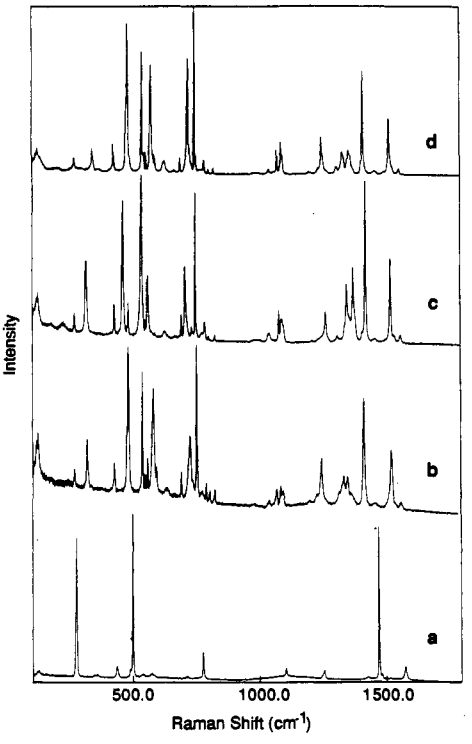

Figure 4. (a) FT-Raman spectrum of C_{60}. (b) FT-Raman spectrum of $(Pt(PEt_3)_2)_6(\eta^2\text{-}C_{60})$. (c) FT-Raman spectrum of $(Pd(PEt_3)_2)_6(\eta^2\text{-}C_{60})$. (d) FT-Raman spectrum of $(Ni(PEt_3)_2)_6(\eta^2\text{-}C_{60})$.

potentials of the complexes are more negative than found for C_{60}.[13] The X-ray crystal structures of metal complexes also indicate substantial backbonding near the metal-binding site.[6,7,14]

The infrared spectra are, unfortunately, not as simple as the Raman spectra. The phosphine ligands possess very strong infrared absorptions, while the allowed infrared C_{60} vibrational modes are relatively weak; the triphenylphosphine modes dominate the infrared spectrum. The $Pt(PPh_3)_2(\eta^2\text{-}C_{60})$ complex shows strong perturbations of the phosphine modes resulting in frequency shifts from the model compound $Pt(PPh_3)_2Cl_2$ which makes identification of the new C_{60} modes impossible at this time.

Further substitution on the C_{60} sphere has now been achieved and the hexasubstituted nickel, palladium, and platinum complexes $[Ni(PEt_3)_2]_6C_{60}$, $[Pd(PEt_3)_2]_6C_{60}$, and $[Pt(PEt_3)_2]_6C_{60}$ are available. X-ray studies have established the symmetry as approaching T_h (the phosphine ligands tip slightly out of the plane defined by the metal and the two bonded carbons).[14] If the C_{60} sphere is still relatively undistorted, then the number of observed modes should be intermediate between those of the parent C_{60} molecule and the monosubstituted complexes already discussed. The FT-Raman spectra of the three complexes along with the reference spectrum of C_{60} are shown in Figure 4. The correlation of the original C_{60} modes and the new observed modes in the complexes is less clear than found for the monosubstituted complexes. Significant electron donation through π backbonding has shifted the frequencies sufficiently that the modes no longer resemble pure C_{60} vibrations. The X-ray crystal structure[14] shows

(13) Lerke, S.; Evans, D.; Fagan, P. J.; Parkinson, B. Unpublished data.
(14) (a) Fagan, P. J.; Calabrese, J. C.; Malone, B. *J. Am. Chem. Soc.* **1991**, *113*, 9408. (b) Fagan, P. J.; Calabrese, J. C.; Malone, B. *Acc. Chem. Res.* **1991**, in press.

significant distortions along the three orthogonal axes defined by the three pairs of metal centers. It is, however, clear that the high-frequency modes at 1470 and 1570 cm^{-1} have been shifted to lower frequency by 30 cm^{-1} as opposed to less than 10 cm^{-1} for the monosubstituted systems. This is consistent with the increased π backbonding brought on by the six metal centers.

In conclusion, the Raman spectra of organometallic complexes involving C_{60} provide a clear probe into the symmetry reduction upon reaction of the C_{60} molecular system. This reduction in symmetry results in the observation of both "silent" modes and the splitting of degenerate modes in the Raman spectrum. As the degree of substitution is increased, the perturbations of the C_{60} vibrational modes become stronger and the correlations with the original vibrational spectrum of the parent become less clear. The spectra reported here should be useful benchmarks in characterizing structurally related C_{60} derivatives.

Acknowledgment. We acknowledge the assistance of B. Malone and E. Holler for the synthesis and purification of C_{60}.

Communications to the Editor

Synthesis and Conformational Analysis of GM_3 Lactam, a Hydrolytically Stable Analogue of GM_3 Ganglioside Lactone

Asim K. Ray, Ulf Nilsson, and Göran Magnusson*

Organic Chemistry 2, Chemical Center
Lund Institute of Technology, University of Lund
P.O. Box 124, 221 00 Lund, Sweden

Received November 12, 1991

Gangliosides have been found to occur in conjunction with the corresponding lactones (e.g., **1**) in brain tissue[1] and in the membranes of tumor cells.[2] The lactones are unstable at neutral pH. We now report the synthesis of the stable lactam **3** and derivatives corresponding to the natural GM_3 lactone. The conformations of **1** and **3** are similar, thus making the lactams potential substitutes for ganglioside lactones in biomedical research. The lactams might be natural products yet to be discovered.

The lactone of GM_3 ganglioside (**1**, "GM_3 lactone") has been suggested to be a tumor-associated antigen on cells of an experimental mouse melanoma.[2] In a comparative immunization with GM_3 ganglioside and **1**, it was shown that the latter was the stronger immunogen, and it was suggested that it could be the real immunogen despite being a minor membrane component.[2] The reactivity of a monoclonal anti-melanoma antibody (M2590) with various cells and liposomes was shown[2] to depend in a threshold, all-or-none fashion on the concentration of GM_3 ganglioside in the cell membrane or liposome. The antibody was found to cross-react with **1**.

Acidic conditions favor the lactone in the equilibrium GM_3 ganglioside $\rightleftarrows$ GM_3 lactone.[3] Since GM_3 ganglioside is an acidic glycolipid, it might induce its own lactonization when the concentration is high in a cell membrane or liposome. This can help to explain the threshold effect described above and may have implications for other sialic acid-containing saccharides.

The equilibrium concentration of GM_3 lactone is low at close-to-neutral pH, and it may therefore be a rather inefficient immunogen. In contrast, the corresponding lactam (cf. **3**, "GM_3 lactam") is perfectly stable at neutral pH and should be a good lactone substitute, provided that the overall shape of lactone and lactam is similar. We report the synthesis and conformational analysis of the 2-(trimethylsilyl)ethyl[4] (TMSEt) glycoside of GM_3 lactam **3** as well as the spacer glycoside **11** and the neoglycoprotein **12**.

The TMSEt 2′-azidodeoxylactoside **4** {$[\alpha]^{22}_D$ +19° (*c* 1, $CDCl_3$); ^1H NMR δ 4.40, 4.31 (H-1,1′)} was synthesized in 37% overall yield by glycosylation of 2-(trimethylsilyl)ethyl 2,3,6-tri-*O*-benzyl-β-D-glucopyranoside[4] with 3,4,6-tri-*O*-acetyl-2-azido-2-deoxy-α-D-galactopyranosyl bromide[5] followed by deacetylation, formation of the 3′,4′-acetonide, benzylation of the 6′-position, and removal of the acetonide group. Glycosylation of **4** with the *N*-acetylneuraminic acid derivative **5**[6] according to the method of Lönn et al.[7] gave the trisaccharide derivative **6** in high yield {71%, $[\alpha]^{22}_D$ −13° (*c* 1, $CDCl_3$); ^1H NMR δ 4.50, 4.40 (H-1′,1)} together with the β-anomer (4%). The α-configuration of **6** was determined by NMR[8] spectroscopy ($J_{C1-H3ax}$ = 6.15 Hz). Nickel boride ($NaBH_4/NiCl_2{\cdot}6H_2O/H_3BO_3$) reduction of **6**, O-deacetylation of the resulting crude amine, treatment with pyridine to effect the lactam ring closure, and hydrogenolysis of the benzyl protecting groups gave **3** {54%, $[\alpha]^{22}_D$ −22.3° (*c* 0.7, MeOH); ^1H NMR δ 4.69, 4.47 (H-1′,1), 4.32 (H-4″), 3.23 (H-2), 2.59 (H-3″eq), 2.02 (NHAc), 1.67 (H-3″ax); *m/z* calcd for $C_{28}H_{51}O_{17}N_2Si$ (M + H) 715.2957, found 715.2958} after chromatographic purification. Compound **3** was acetylated to give **7** {98%, $[\alpha]^{29}_D$ −32° (*c* 0.8, $CDCl_3$); ^1H NMR δ 4.54, 4.40 (H-1,1′)}. The TMSEt glycoside **7** was transformed[9] into the α-chloro derivative **8** [100%; ^1H NMR δ 6.20 (H-1)]. Glycosylation of 2-bromoethanol with **8** gave the 2-bromoethyl glycoside **9** {54%, α/β 15:85; $[\alpha]^{25}_D$ −27° (*c* 1.2, $CDCl_3$); ^1H NMR δ 4.78 (H-1′)}. Glycoside **9** was treated[10] with methyl 3-mercaptopropionate to give **10** {82%, $[\alpha]^{22}_D$ −23° (*c* 1.1, $CDCl_3$); ^1H NMR δ 4.63 (H-1′), 3.69 (COOMe)}. Deacetylation of **10** gave the spacer glycoside **11** {86%, $[\alpha]^{25}_D$ −0.1° (*c* 0.5, MeOH); ^1H NMR δ 4.92, 4.69, 4.48 (H-1α, H-1′, H-1β)}, which was used for coupling[10] to bovine serum albumin to give the neoglycoprotein **12** (~21 mol of **11** per mol of BSA according to sulfur analysis[10]), useful as an antigen for immunization purposes (Scheme I).

A conformational analysis of GM_3 lactone (**1**), based on NMR data, was reported by Yu et al.[11] A highly rigid structure was proposed, where the lactone ring occupies a chairlike conformation. However, we suggest that a boatlike conformation is instead preferred: (i) both the lactones (**1** and **2**[12]) and the lactam (**3**) show a deshielding of H-4″ as compared to the open-form GM_3 ganglioside (δ 3.55 for GM_3 ganglioside and 4.12 for **1**, both in

(1) Gross, S. K.; Williams, M. A.; McCluer, R. H. *J. Neurochem.* **1980**, *34*, 1351-1361.
(2) Nores, G. A.; Dohi, T.; Taniguchi, M.; Hakomori, S.-I. *J. Immunol.* **1987**, *139*, 3171-3176.
(3) Wiegandt, H. *Ergeb. Physiol. Biol. Chem. Exp. Pharmacol.* **1966**, *57*, 190-222.
(4) Jansson, K.; Ahlfors, S.; Frejd, T.; Kihlberg, J.; Magnusson, G.; Dahmén, J.; Noori, G.; Stenvall, K. *J. Org. Chem.* **1988**, *53*, 5629-5647.
(5) Lemieux, R. U.; Ratcliffe, R. M. *Can. J. Chem.* **1979**, *57*, 1244-1251.
(6) Marra, A.; Sinaÿ, P. *Carbohydr. Res.* **1989**, *187*, 35-42.
(7) (a) Birberg, W.; Lönn, H. *Tetrahedron Lett.* **1991**, *32*, 7453-7456; 7457-7458. (b) Lönn, H.; Stenvall, K. *Tetrahedron Lett.* **1992**, *33*, 115-116.
(8) Hori, H.; Nakajima, T.; Nishida, Y.; Ohrui, H.; Maguro, H. *Tetrahedron Lett.* **1988**, *29*, 6317-6320.
(9) Jansson, K.; Noori, G.; Magnusson, G. *J. Org. Chem.* **1990**, *55*, 3181-3185.
(10) Dahmén, J.; Frejd, T.; Magnusson, G.; Noori, G.; Carlström, A.-S. *Carbohydr. Res.* **1984**, *127*, 15-25; *127*, 27-33; *129*, 63-71.
(11) Yu, R. K.; Koerner, T. A. W.; Ando, S.; Yohe, H. C.; Prestegard, J. H. *J. Biochem.* **1985**, *98*, 1367-1373.
(12) Gift from Dr. J. Dahmén, Symbicom AB, Ideon Research Park, Lund, Sweden.

0002-7863/92/1514-2256$03.00/0